



The assessment of an acoustic Doppler velocimetry profiler from a user's perspective

Da Liu¹ · Khaldoon Alobaidi¹ · Manousos Valyrakis¹

Received: 7 August 2021 / Accepted: 1 July 2022 / Published online: 31 August 2022
© The Author(s) 2022

Abstract

Acoustic Doppler velocimetry profilers (ADVPs) are widely used in both experimental and field studies because of their robustness in velocity measurements. The acquired measurements do not only offer estimates of the local and instantaneous flow velocity at the interrogated measurement volume, but can also be further processed for the estimation of the bed surface shear stresses, thus they are finding a wide range of applications ranging from water engineering to geomorphology and eco-hydraulics. This study aims to evaluate the performance of an ADVP in obtaining hydrodynamics measurements under fixed flow conditions, with various probe configurations. To this goal, a robust search is conducted where ADVP probe settings are sequentially altered. A number of assessment criteria are used including qualitative observations, such as checking the shape of the velocity profile, as well as quantitative error metrics, including signal-to-noise ratio, correlations and number of spikes. Further, estimation of the bed shear stresses computed by means of using the log Law of the Wall and turbulent kinetic energy, allow obtaining a better understanding of the uncertainties involved and the importance of making a better informed choice with respect to the probe configuration settings. Thus, the methodology and performance metrics provided herein, although presented for a given flow, can generally be applied from practitioners and researchers alike.

Keywords Acoustic Doppler velocimetry profilers · Flow velocity · Shear stress · Turbulent kinetic energy · Turbulence

Introduction

Acoustic Doppler velocimetry (ADV) is widely used as one of the most versatile and robust flow diagnostics tools for both laboratory and field studies across a range of research and applied themes spanning engineering eco-hydraulics and geomorphology. A range of specific ADV probes with varying specifications are readily available for use by professionals and researchers. ADV measures the sampling volume of a water body in the water flow via the Doppler shift caused by the reflection of the pulse transmitted from the centre transducer (the centre beam) and received by the four receiving beams (Nortek 2012; NortekAS 2015; Kraus et al. 1994). An acoustic Doppler velocimetry profiler (ADVP),

i.e. Vectrino II, has the same working principle, but enables profile measurements, which may involve interrogating more than one measurement points, at the same time. Thus, ADVPs may typically have additional parameters that the user may need to define in the probe settings, which even though desirable, may leads to increased uncertainties if there is no generally acceptable guidance to enable their optimal use.

Many research works about the noise associated with acoustic signal of ADV have been done, such as Khorsandi et al. (2012), García et al. (2005), Anderson and Lohrmann (1995). It is suggested that Doppler noise might increase the value of flow hydrodynamics computed by time series of instantaneous velocities, such as turbulence intensities and turbulent kinetic energy (Anderson and Lohrmann 1995). Signal-to-noise ratio (SNR), as an important indicator of data quality, is defined as $SNR = 20 \log_{10} \left(\frac{\text{Amplitude}_{\text{signal}}}{\text{Amplitude}_{\text{noise}}} \right)$, and it is given the unit of dB (Nortek 2012). SNR sweet spot, where the measurement has the highest SNR is located 5 cm below the transmitter (Nortek 2012). At the same time, the correlations between the successive pings are suggested to be above 90% (NortekUSA 2011).

Edited by Dr. Łukasz Przyborowski (GUEST EDITOR) / Dr. Michael Nones (CO-EDITOR-IN-CHIEF).

✉ Manousos Valyrakis
Manousos.Valyrakis@glasgow.ac.uk

¹ Water Engineering Lab, School of Engineering, University of Glasgow, Glasgow G12 8QQ, UK

A wide range of post-processing methods have been developed for velocity time series to improve the performance of ADV. Some of these methods are numerical analyses of the time series, and some of them involve indicators of data quality like SNR and correlations (Goring and Nikora 2002; Parsheh et al. 2010; Hurther and Lemmin 2001; Jesson et al. 2013, 2015). Most of these methods introduce removing or replacing the spikes. In fact, any post-processing algorithm may influence the integrity of the velocity representation. Compared to post-processing the velocity time series, enhancing the data quality during recording is also important to enhance the data quality (Voulgaris and Trowbridge 1998). To achieve this, some studies have identified the relation between Doppler acoustic seeding material and Doppler noise, as an inherent factor of this technique (Khorsandi et al. 2012).

Certain hydrodynamics measurements taken by ADVP (Vectrino II) are compared with other flow velocity measuring equipment, such as PIV and ADV, like Vectrino I, (Zedel and Hay 2011; Craig et al. 2010). Near bed measurements taken by ADVP may be influenced by the bottom echo, and may be associated with very high SNR, which can hardly reflect the flow velocity (Rusello 2012). Vectrino I has been used in recording flow velocities over a few decades. Vectrino II, as an updated version of Vectrino I, is more customised, and it enables the highest frequency of 100 Hz, which can better represent the flow hydrodynamics. However, in practice using ADVP under certain default configurations can easily result in obtaining flow diagnostics that are non-representative of the real flow conditions. This appears to be true for most probe settings but even more so for those with which higher temporal resolution can be achieved. Vectrino II has a few indexes in the probe configuration, and different probe settings can influence the velocity result to some extents. In order to identify the best probe configuration, a number of velocity profiles are taken at the same location of a flume, under the same flow rate, but with different probe configurations.

Methods

Preliminary observations in using this probe revealed that there is a varying level of dependency on a number of parameters in the probe configuration, which are not detailed in the user manual, and lack a definite guide for the user. Subsequently users of this equipment may end up underutilizing or using it in a manner that returns inaccurate results. To this goal a series of laboratory experiments have been conducted, under the same open channel flow conditions, using a profiler (ADVP Vectrino II from Nortek®) aiming to cover the full range of probe configuration combinations that can be used in practice. Flow velocities have been measured

via the software Nortek Multi-Instrument Data Acquisition System (Vectrino Profiler). The operation of the probe is configured via the configuration panel at the probe's proprietary software and is governed by a range of parameters (Fig. 1). For this study a range of values for the configuration parameters are chosen to be tested, so that their impacts on flow diagnostics can be identified.

The experiment has been conducted in a recirculating glass walled flume with sufficient length (> 10 m) in the Water Engineering Laboratory at the University of Glasgow. A series of acrylic panels are placed on the side of the flume with an angle of 17° to simulate riverbank (Fig. 2). It is also shown in Fig. 2 that a vegetation array consist of some acrylic rods (with a uniform diameter of 6 mm, spaced 160 mm each other and configured linearly) are placed on the top of the riverbank via a series of support panels, starting from 4.5 m upstream of the measurement location. The width of the main channel is 1 m, and the flume bed consists of a few centimetres high layer of sand with nominal diameter from 0.5 to 2.36 mm ($d_{50} = 1$ mm) covering the whole flume width (Fig. 2). The sand bed is designed to be fixed during all experiment runs. The velocity profiles have been taken at the same location (6 m downstream of the inlet, and 345 mm away from the sidewall; the measurement location is denoted by a red bar in Fig. 2) under the exactly same flow conditions, but different probe configurations. The flow rate

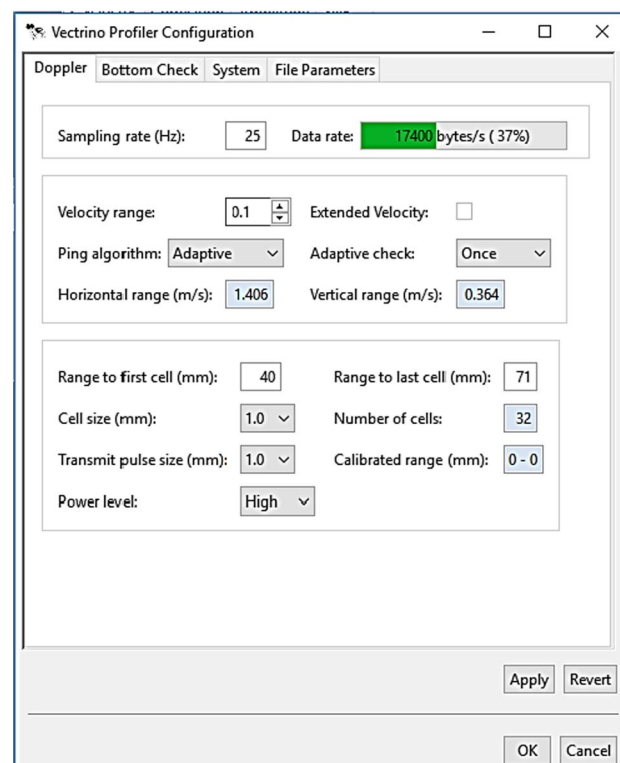
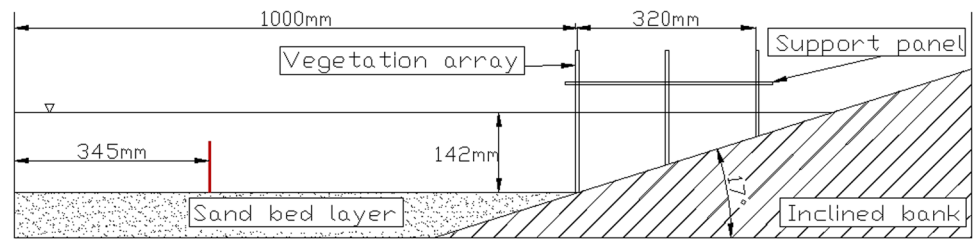


Fig. 1 Probe configuration window in Vectrino Profiler

Fig. 2 Cross-sectional view of the experimental flume, the vertical red bar denotes the location of velocity profile measurements



is about $0.0105 \text{ m}^3/\text{s}$, which is calculated from the average measurements of electromagnetic flow meters attached to the inlet pipes via which water is circulated in the flume. The flow depth is constantly equal to 142 mm along the flume length, which results in a mean flow velocity of about 0.060 m/s. The Reynolds number is about 7000, and the flow is turbulent and the turbulent boundary layer is fully developed at the measurement cross section.

The probe is joined with a vertical gauge, which enables the probe to move vertically. The measurement height can be measured by using the bottom check function of Vectrino II. For each experiment, single or profile (measuring multiple points at one time) measurements have been taken to reconstruct a velocity profile. While taking the velocity profiles, the probe has been adjusted to different heights so that the measurement locations correspond to the specific flow depth as shown in the velocity profile plots. Given that the flow assessed herein is statistically the same along the longitudinal direction, and given that the probe's geometry remains fixed, we expect there is no effect on the flow measurements. An effort is applied in keeping the orientation of the probe as consistent as possible and aligning vertically to the main flow direction. Some preliminary tests show that the velocity time series longer than 1 min has negligible errors in both mean velocity and standard deviation. So, depending on various frequencies, with the minimum measurement time

is 1 min, about 6000 samples were constantly exerted in the velocity time series for all configurations. For instance, the probe records velocity for 1 min at a sampling rate of 100 Hz, and records velocity for 4 min at a frequency of 25 Hz. In addition, a velocity profile taken by ADV (Vectrino I) is also presented in this study, for reference.

The effect of tested parameters, including profile length (is shown in Fig. 3, adjusted by Range to first cell and Range to last cell), Sampling rate, Ping algorithm, Transmit pulse size and Cell size, on the sensitivity and the accuracy of the obtained results is assessed. The range of values that is chosen for the test indexes are given in Table 1. This initial assumption of the values of the parameters is made according to the user manual and after preliminary tests. Only one index is changed each time, which allows for checking the effect of each of those indexes on the velocimetry results. A naming system is devised by a combination of six digits, which denotes the value of the aforementioned parameters (Table 1). For instance, 213,211 means that a 10 mm long profile, which consists of 10 cells at one measurement, with both Transmit pulse size and Cell size of 1 mm measuring the velocity at 100 Hz, and it has Max interval Ping algorithm, and starts at 40 mm below the probe centre beam. Those with 'Single' as Profile length indicates that the probe measures only one point at one measurement, which is defined as point measurements, and its actual length

Fig. 3 Schematic drawing of the working principle of ADVP, with showing of Range to first cell, Range to last cell and Profile length

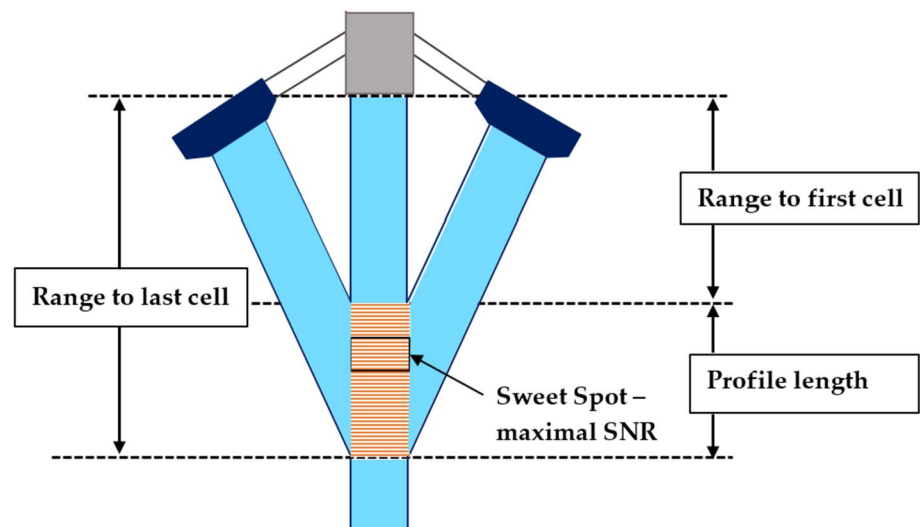


Table 1 Naming system used in this experiment

	First digit				Second digit		Third digit			Fourth digit		Fifth digit				Sixth digit			
	Profile length (mm)*				Range to first cell (mm)		Sampling rate (Hz)			Ping algorithm		Transmit pulse size (mm)				Cell size (mm)			
# in Naming	1	2	3	4	1	2	1	2	3	1	2	1	2	3	4	1	2	3	4
Value	Single	10	20	30	40	50	25	50	100	Adaptive	Max interval	1	2	3	4	1	2	3	4

*‘Profile length’ is basically the value of Range to last cell minus the value of Range to first cell, ‘Single’ indicates point measurements. The actual length may differ with the number shown here for profile measurements, and it will be the nearest integer number, which is smaller than the displayed value

is dependent on the length of the Cell size (cell size and pulse length are usually the same for two pulse-coherent method, but the larger cell sizes can be obtained by averaging the pulse length returns at different depths). The elevation of the middle point of the sampling volume denotes the height of the velocity measurement.

The experiment has been conducted in two phases. In the preliminary phase, the maximum and the minimum value of each index are chosen, respectively, to consist of 48 profiles. Because the restrain due to the water depth, probe configurations with profile length of 30 mm and Range to first cell of 50 mm can only take two profiles, and these probe configurations are not experimented. After acquiring the velocity profiles in this phase, a visual check has been done (details can be seen in the next section). The result clearly showed that Adaptive Ping algorithm always lead to random results (extremely high errors), where the detail can be seen from Table 2. Similar findings also can be found in (Rusello 2012). So the Ping algorithm should be fixed to be Max interval in the refined phase of the experiment. With additional considerations of the results from the preliminary phase, Range to first cell can be fixed to 40 mm, because very small variations have been found in this phase, and Transmit pulse size and Cell size are changed correspondingly. Then, in the refined phase, other values of the index are tested in a similar way, which consisted of another 12 probe configurations.

Results

All results are processed to velocity profile analysis, including visual check and fitness check to a standard logarithmic function. The results of velocity profiles with qualified logarithmic shape are then processed to shear stress and turbulent kinetic energy analyses. Some spikes occur in the time series due to the inherent problems of the measuring technology or insufficient seeding material for specific probe configurations. So all velocity time series obtained in this study are despiked as it is described in (Goring and Nikora

2002), and the identified spikes are removed. The impact of spikes on the result is discussed separately.

Velocity profiles

By visually checking the velocity profile plots, the results obtained from the preliminary phase are identified as ‘smooth’ (Fig. 4a, b), ‘curved’ (Fig. 4c) and ‘random’ (Fig. 4d). It can be seen that all measurements with Adaptive Ping algorithm are identified as random. The influence of echoes from boundaries can affect the result up to approximately 10 mm above the sand bed (up to the 5th point from the bed in the profile). Different from smooth and curved profiles, at the near bed region of random profiles, the velocity varies a lot (111144 and 113141 in Fig. 4d). Even from observation the magnitude of velocity for the smooth profiles varies up to 25% (Fig. 4a, b). Figure 3c shows that many profile measurements result in curved velocity profile shape in each profile measurement. For example, experiment 411241 and 411214 (Fig. 4c) only show an abnormally small velocity at the near bottom portion of each profile, but experiment 411211, 413211 and 413241 (Fig. 4c) show the highest velocity at the sweet spot (50 mm below the centre beam, Fig. 3) and abnormally smaller velocity at distal to the sweet spot (Fig. 4c).

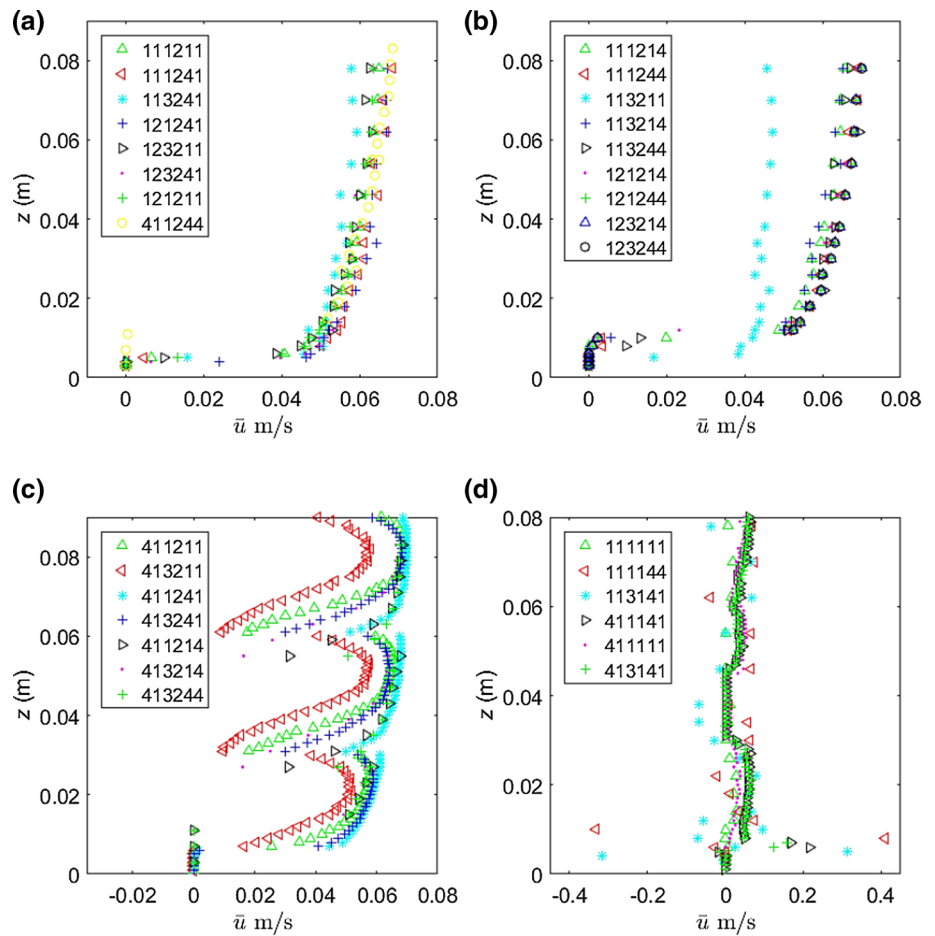
Some additional quantitative analyses of the velocity profiles by assessing their fitness to logarithmic functions are also taken to assess the quality of the velocity profile. Velocity profiles are plotted in log scale to see how they fit a line of $\bar{u} = p_1 x \log(z) + p_2$ where z denotes the elevation of velocity measurement, \bar{u} denotes the time-averaged velocity, p_1 and p_2 identify the slope of the function and its intersection to the axis, respectively. The first five points from the bed are not taken into account for analysing, because the result are influenced by the strong echo from the boundary as it has been mentioned before. Some indicators are involved in the function fitness check stage, including sum of squared errors (SSE, defined by Eq. 1), coefficient of determination (R^2 , defined by Eqs. 2 and

Table 2 Summary of the velocity profile analysis in the preliminary phase, SNR and correlations are also shown in this table

Experiment	p_1	p_2	SSE	R^2	RMSE	SNR (dB)	Correlations (%)	Visual check
111111	- 8.982	- 1.406	0.980	0.098	0.286	26.1	96.3	Random
111114	4.593	- 1.602	1.036	0.046	0.294	28.9	96.2	Random
111141	2.339	- 1.641	0.926	0.148	0.278	26.9	77.4	Random
111144	1.301	- 1.535	0.840	0.227	0.265	33.2	84.2	Random
111211*	55.080	- 4.704	0.008	0.993	0.026	12.0	81.0	Smooth
111214	20.280	- 2.654	0.366	0.663	0.175	21.9	90.6	Smooth
111241*	56.751	- 4.952	0.030	0.972	0.050	12.1	80.9	Smooth
111244	12.928	- 2.261	0.492	0.547	0.202	28.3	95.4	Smooth
113111	- 2.604	- 1.503	1.084	0.002	0.301	25.3	95.2	Random
113114	7.761	- 1.700	0.887	0.184	0.272	29.0	95.3	Random
113141	- 1.258	- 1.499	1.016	0.065	0.291	26.3	81.8	Random
113144	- 1.027	- 1.459	1.063	0.021	0.298	32.5	89.4	Random
113211	134.550	- 7.530	0.401	0.631	0.183	9.8	73.1	Smooth
113214	14.211	- 2.295	0.503	0.537	0.205	23.6	90.6	Smooth
113241*	74.683	- 5.570	0.139	0.872	0.108	12.7	82.9	Smooth
113244	15.906	- 2.433	0.467	0.571	0.197	29.5	95.1	Smooth
121114	13.211	- 1.978	0.673	0.380	0.237	27.2	96.4	Random
121141	0.148	- 1.524	1.086	0.000	0.301	21.1	80.5	Random
121144	4.138	- 1.706	0.750	0.310	0.250	29.5	88.5	Random
121214	12.229	- 2.190	0.359	0.669	0.173	25.8	94.8	Smooth
121241*	50.742	- 4.591	0.044	0.959	0.061	14.8	91.7	Smooth
121244	12.490	- 2.245	0.501	0.539	0.204	28.2	95.6	Random
123111	- 1.616	- 1.488	1.083	0.004	0.300	20.6	94.7	Random
123114	22.750	- 2.272	0.329	0.698	0.165	24.7	94.7	Random
123141	- 0.550	- 1.491	1.078	0.008	0.300	19.5	82.8	Random
123144	1.623	- 1.611	0.992	0.087	0.288	28.1	89.4	Random
123211*	58.639	- 4.856	0.062	0.943	0.072	13.6	87.1	Smooth
123214	13.776	- 2.276	0.458	0.578	0.195	23.9	91.9	Smooth
123241*	56.597	- 4.811	0.057	0.948	0.069	13.6	88.9	Smooth
123244	13.023	- 2.253	0.460	0.576	0.196	27.4	94.6	Smooth
121111	5.010	- 1.617	1.037	0.045	0.294	21.7	95.5	Random
121211*	53.445	- 4.570	0.033	0.970	0.052	14.5	87.7	Smooth
411111	9.327	- 1.675	5.714	0.224	0.262	9.1	76.0	Random
411211	8.406	- 1.841	5.941	0.193	0.268	7.1	58.7	Curved
411141	- 3.172	- 1.266	6.532	0.113	0.281	16.5	84.9	Random
411241	25.354	- 2.977	2.845	0.614	0.185	11.9	81.3	Curved
413111	7.363	- 1.594	6.148	0.165	0.272	10.8	75.5	Random
413211	5.690	- 1.628	6.690	0.091	0.284	6.9	66.0	Curved
413141	- 3.701	- 1.252	6.602	0.103	0.282	16.3	83.9	Random
413241	13.324	- 2.149	5.521	0.250	0.258	11.1	81.1	Curved
411114	4.960	- 1.496	0.588	0.119	0.186	16.0	88.0	Random
411214	7.096	- 1.749	0.544	0.185	0.179	14.3	77.4	Curved
411144	2.295	- 1.433	0.638	0.043	0.194	24.6	94.4	Random
411244*	42.594	- 4.000	0.028	0.957	0.041	23.0	92.6	Smooth
413114	7.855	- 1.582	0.350	0.475	0.144	15.8	85.4	Random
413214	3.387	- 1.506	0.606	0.092	0.189	13.7	79.2	Curved
413144	3.040	- 1.462	0.602	0.098	0.188	23.2	92.8	Random
413244	23.145	- 2.750	0.309	0.537	0.135	21.8	91.2	Curved

Profile numbers in bold indicates the good-fit results (low SSE, low RMSE and high R^2)

Fig. 4 Velocity profiles of selected experiments. **a** ‘smooth’ from the visual check and good-fit a logarithmic function, **b** ‘smooth’ from visual check, **c** ‘curved’ from visual check, **d** ‘random’ from the visual check



3), and root-mean-square error (RMSE, defined by Eq. 4). SSE is defined as:

$$SSE = \sum_{i=1}^K (\bar{u}_i - \hat{u}_i)^2, \tag{1}$$

where K denotes the total number of velocity points in the velocity profile; \bar{u}_i denotes the time-averaged velocity; \hat{u}_i is calculated from the best-fit logarithmic function by using the corresponding elevation. R^2 is defined by Eqs. 2 and 3:

$$\bar{U} = \frac{1}{K} \sum_{i=1}^K \bar{u}_i \tag{2}$$

$$R^2 = 1 - \frac{\sum_{i=1}^n (\bar{u}_i - \hat{u}_i)^2}{\sum_{i=1}^n (\bar{u}_i - \bar{U})^2}, \tag{3}$$

where \bar{U} denotes the profile mean velocity, n is number of samples in each velocimetry record, and K is the total number of velocity measurements in the velocity profile. R -squared closer to 1 means that the velocity profile has

a better regression fit to its best-fit logarithmic function. RMSE is defined as:

$$RMSE = \sqrt{\frac{\sum_{i=1}^n (\bar{u}_i - \hat{u}_i)^2}{n}}. \tag{4}$$

RMSE describes the error in addition to SSE with considerations of the number of velocity points in the velocity profile.

Some errors are extremely high because of those random results (Table 2). The median value of each error indicator is chosen as the critical value. In other words, the first 50% among all profiles from low error to high error for the specific indicator are processed for the next step. Those profiles meet the critical value of all these three error indicators are identified as good-fit results. Profile names marked with ‘*’ indicated the good-fit profiles, which are plotted in Fig. 4a.

It can be seen from Table 2, that all good results from logarithmic function check are parts of ‘smooth’ profiles identified by visual check. The results of the preliminary phase show that the average SSE, R^2 and RMSE are 1.75, 0.15 and 0.26 for all Adaptive Ping algorithm, and are 1.12, 0.62 and 0.15 for all Max interval Ping algorithm. R^2 as an indicator of the regression of the profile shape to a standard

logarithmic function is very small for Adaptive Ping algorithm, which indicates that the profile shape can be non-logarithmic shape, consistent to the of visual check results. Random velocity profiles are also observed in Thomas et al. (2017).

Even among the good-fit results, the values of y_1 and y_2 vary a lot, which means the logarithmic shape that they follow is different, which can significantly influence the near bed shear stress estimation, for example done under the log Law of the Wall assumption. However, both the magnitude and the shape of the stream-wise velocity profiles with different Range to first cell are generally the same (i.e. 111211 and 121211; 113241 and 123241 have similar p_1 and p_2). In the refined phase is fixed to 40 mm below the centre beam, which reduces restraints due to the flume geometry, and enables more measurements. According to the instruction by the probe manufacturer, the Transmit pulse size and the

Cell size should normally correspondingly change, and no clear impact of the correlations between these two parameters is observed in the preliminary experiment phase, so in the refined phase, these two indexes are changed correspondingly to the same value.

Most velocity profiles obtained in the refined phase are identified as smooth by visual check, except experiment 212222 and 311222, where clear gaps between the two distal ends of each profile measurement can be observed (Fig. 5). The strong echo from the boundary causes near zero result until about 0.01 m above the bed for most measurements. Larger cell size may lead to longer boundary affected region (e.g. profile 311244 and 312244 in Fig. 5), as the midpoint of the cell is considered as its elevation in this plot. The velocity profile obtained by Vectrino I is also smooth, but it clearly follows a different logarithmic shape comparing with those of most good results taken by Vectrino II. Similar function checks are applied to refined phase as well, and the results are shown in Table 3. The overall quality of results for the refined phase is much higher than it for the preliminary phase, so the same reference values of SSE, R^2 and RMSE used in the preliminary phase are applied, and the results are given in Table 3.

Most good-fit profiles by function check are smooth, unless experiment 211222 and 311222. Though these profile are good-fit of the logarithmic function, it can hardly use in research studies, because clear biases exist between each profile measurement. From a view of all good-fit results among the whole test, p_1 and p_2 vary from approximately 19–75, and from approximately – 6 to – 2.6, respectively. These indicate that both the logarithmic function and its intersection to the axis may have quite big variations, which can be reflected in the magnitude of the shear stress estimated by the log Law of the Wall and the computed

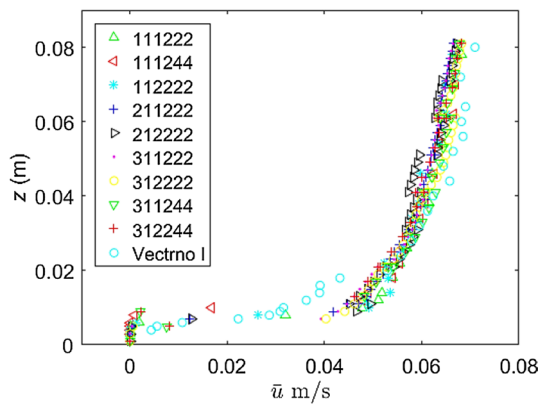


Fig. 5 All velocity profiles obtained in the refined experiment phase and the velocity profile taken by ADV (Vectrino I)

Table 3 Summary of the results obtained in the refined phase

Experiment	p_1	p_2	SSE	R^2	RMSE	SNR (dB)	Correlations (%)	Visual check
Vectrino I*	48.884	- 6.219	0.396	0.956	0.148	16.1	86.9	Smooth
111,222*	46.487	- 4.242	0.013	0.988	0.033	21.9	93.4	Smooth
111,233	21.229	- 2.726	0.337	0.690	0.168	27.5	95.0	Smooth
111,244*	18.831	- 2.573	0.319	0.706	0.163	29.7	95.6	Smooth
112,222*	48.542	- 4.316	0.051	0.953	0.065	19.2	88.7	Smooth
112,233	21.081	- 2.720	0.332	0.695	0.166	26.3	93.0	Smooth
112,244	14.615	- 2.329	0.470	0.567	0.198	28.4	95.1	smooth
211,222*	42.764	- 3.948	0.025	0.990	0.025	24.4	95.0	Smooth
212,222	41.808	- 3.880	0.158	0.938	0.062	24.5	94.5	Curved
311,222	39.450	- 3.735	0.057	0.973	0.039	17.6	93.6	Curved
312,222*	36.791	- 3.628	0.042	0.980	0.034	17.8	92.8	Smooth
311,244*	42.680	- 4.006	0.025	0.960	0.038	26.7	95.8	Smooth
312,244*	35.543	- 3.508	0.007	0.989	0.020	26.4	95.7	Smooth

Profile numbers with bold and ‘**’ denote the good-fit (low SSE and low RMSE and high R^2) results in this research phase

Nikuradse's equivalent sand roughness. Further analyses by using the log Law of the Wall is needed, and are introduced in "Near bed shear stress".

SNR

SNR and Correlations can indicate the data quality of the velocity time series with considerations of Doppler noise level. Despite Correlations remains good for most measurements, Vectrino II point measurements generally have lower SNR values than those profile measurements and point measurement taken by Vectrino I in the exactly same flow condition. This can be considered as that point-based measurements by Vectrino II need more acoustic recognized seeding in the sampling volume to achieve the same value of SNR. Profile measurements taken by Vectrino II have higher SNR, which generally meet the threshold (at least 30 dB at the sweet spot and 20 dB at the distal) suggested by Nortek for most measurements (NortekUSA 2011). The value of SNR for the Vectrino I is constantly above 18 dB, which is above the threshold of it suggests by many research studies (Khorsandi et al. 2012; McLelland and Nicholas 2000). However, such guidance for point measurements taken by Vectrino II has not been made available yet.

The result also shows that SNR and correlations are not independent of probe configurations. In this experiment, the flow condition remains exactly the same, but the mean SNR varies from 6 to 30 dB, and the mean correlations vary from 58 to 96% (Tables 2 and 3). SNR and correlations indicate the noise level of the measurement, lower SNR and correlations may result in an increase number of spikes of the velocity time series. However, good SNR and correlation do not have direct link to good quality of results (i.e. experiment 111111 and 121114).

Near bed shear stress

Many research studies have used velocity profiles obtained by either ADV or ADVP to estimate the near bed shear stress by using the log Law of the Wall (τ_{\log}). For the same bed roughness and same flow condition, as in this experiment, τ_{\log} should be same for all experiment runs. The impact of various probe settings, based on the profiles that are good-fit to logarithmic functions and τ_{\log} are presented, which can also reflects the shape of the velocity gradient of the profile. Equation 5 is the method introduced in Sumer (2007) which involves Nikuradse's equivalent sand roughness (k_s):

$$\bar{u}(z) = \frac{1}{\kappa} u_* \ln \left(\frac{30(z - z')}{k_s} \right), \quad (5)$$

where κ is the Von Karman constant ($\kappa \approx 0.4$), z denotes the height of the velocity measurement; assuming $z'/k_s = 0.2$

-this value is chosen within the range because it can cover more measuring points in the logarithmic function (Sumer 2007), z' denotes the distance between the tops of the elements comprising the bed surface and the location where the bed shear stress is zero; u_* denotes the shear velocity. Equation 5 can be rearranged to Eq. 6:

$$z - z' = \frac{k_s}{30} e^{\frac{\kappa}{u_*} \bar{u}(z)}, \quad (6)$$

which can be used to acquire u_* and k_s . Similarly, the 5 points close to the bed are not taken into account. Thus, both k_s and u_* can be worked out, and then τ_{\log} can be estimated as: $u_* = \sqrt{\frac{\tau_{\log}}{\rho}}$, where ρ is the water density. According to this method, both k_s and τ_{\log} for all 'smooth' profiles that are good-fit to a logarithmic function are estimated. k_s varies from sub millimetres to 8.7 mm (Table 4). Even the velocity profile is smooth, different probe settings can still influence k_s and τ_{\log} estimations a lot. In this method, the values of u_* and k_s may change correspondingly, and both of these two results are going to be assessed. k_s has been empirically suggested a range of its magnitude, which is well recognised from 1 to 5 times of the median size of the bed material (Sumer 2007; Camenen et al. 2009). The ratio of k_s and d_{50} is presented in Table 4. Generally, k_s obtained by profile-based measurements is higher than it computed by point-based measurement data.

Turbulent kinetic energy (k_t) can be related to near bed shear stress as well. k_t is defined in Eq. 7:

$$k_t = \rho \frac{\overline{u'^2} + \overline{v'^2} + \overline{w'^2}}{2}, \quad (7)$$

where u' , v' and w' denote the fluctuation component of velocity time series of streamwise, transverse and vertical directions, respectively, $\overline{u'^2} = \frac{1}{N} \sum_{i=1}^N (u_i - \bar{u})^2$, \bar{u} is the time-averaged velocity, u_i is the instantaneous velocity. k_t estimation involves u' , v' and w' , which may have higher requirement of the data quality (Voulgaris and Trowbridge 1998). k_t is estimated by using the time series of the three components of the local flow velocity at $z \approx 0.01$ m ($z/h \approx 0.07$), where boundary effects are avoided, and k_t reaches its maximum value (Biron et al. 2004). It can be approximated as $k_t = C_b \rho u^2$, where C_b is a coefficient relevant to bed roughness, and U is the depth mean velocity (Yang et al. 2016). C_b has been estimated by Yang et al. (2016) through both experiment and theory, the obtained values are 0.02 and 0.025, respectively, for the sand bed material with sizes between 0.6 and 2 mm, which is similar to this experiment setup. Among all good-fit velocity profiles, the mean flow velocity estimated by the velocity profile have negligible variations, so U is constantly equal to 0.063 m/s in this study. The bed shear stresses can then be estimated as

Table 4 Summary of τ_{\log} , k_s , τ_{TKE} , and spikes for each experiment with the certain probe configuration

Experiment number	τ_{\log} (Pa)	k_s (mm)	$\frac{k_s}{d_{50}}$	k_t (J/m ³)	τ_{TKE} (Pa)	% of spikes
111211	0.01	0.57	0.57	0.132	0.025	2.8
111241	0.009	0.33	0.33	0.126	0.024	4.1
113241	0.006	0.12	0.12	0.289	0.055	7.2
121241	0.016	0.69	0.69	0.055	0.01	1.2
123211	0.008	0.96	0.96	0.126	0.024	7.2
123241	0.011	0.78	0.78	0.101	0.019	7.2
121211	0.011	0.96	0.96	0.062	0.012	1.9
411244*	0.016	2.46	2.46	0.05	0.01	1.4
Vectrino I	0.026	8.7	8.7	0.278	0.053	0.8
111222*	0.013	1.23	1.23	0.107	0.02	3.4
111244*	0.018	3.81	3.81	0.049	0.009	2.8
112222	0.013	1.35	1.35	0.144	0.027	4.4
211222*	0.015	2.61	2.61	0.084	0.016	1.6
312222	0.022	6.09	6.09	0.048	0.009	1.4
311244	0.018	3.63	3.63	0.041	0.008	1.8
312244	0.022	6.87	6.87	0.04	0.008	1.1

The profile names marked with bold and ‘*’ indicate k_s , τ_{\log} and τ_{TKE} well meet the values estimated from the theory. The results of experiment conducted with Vectrino-I are also shown in this table

$\tau_{TKE} = 0.19k_t$ (Biron et al. 2004; Yang et al. 2016). Turbulent kinetic energy estimated by C_b has been calculated from both of these two values, $0.025\rho u^2$ ($=0.019$ Pa) and $0.020\rho u^2$ ($=0.015$ Pa), and they highly match τ_{\log} estimated for good logarithmic fit profiles (Table 4). Probe configurations that meet both k_s and k_t check are marked with * in Table 4.

Discussion

Physical context and interpretation of the effects of the probe settings

It is generally important to note that as a first consideration, one should always keep in mind the spatiotemporal scales of the relevant flows and the range of fluctuations of the assessed variables, towards making a selection for a velocimetry probe. The research theme of geophysical flows measurement and instrumentation thrives with the implementation of a range of technologies from optical (such as laser Doppler velocimetry or particle image velocimetry) to acoustics and ultrasonics. Consideration of the flow scales and the physical application to being examined will help assess the best technology for each case. As an example, for the low mixing, wall bounded steady flow tried herein ($U \ll 1.2$ m/s), the Vectrino II ADVP has been used. It is noted that for applications with relatively higher flows (e.g. $U \gg 1$ m/s), different velocimetry probes may be preferable. Even though the production of this ADVP has been discontinued, the similar experiments can be conducted with more modern probes (such as Ubertone’s ADVP). It is also

important to note that bi-static Doppler Velocimetry profilers using a narrow-band pulse-coherent technology are limited by the maximum velocity profile range. Broadband incoherent technologies overcome this issue (as testing of more recent acoustic probes from Ubertone has demonstrated, e.g. Conevski et al. 2020). Despite these apparent limitations, the results and observations presented herein are useful both in terms of the general search framework applied towards validating produced ADVP data using sound first principles, as well as a best practice guide for current users of the Vectrino II ADVP probe.

The spatiotemporal resolution and accuracy of point or profile measurements depend on the shape and size of the measurement volume, which in turn is defined by the orientation of the acoustic emitting beams (which are fixed for a given probe) and the probe settings being selected. Vectrino II has a projected beam that becomes wider with the distance from the face of the emitter. This implies that profile measurements at cells more distant from the transducer will be contaminated (due to the receiver probing velocity from adjacent cells), resulting in relatively more erroneous measurements. This is avoided from recently produced devices that have a narrower beam and wider receiving beams, resulting in more focused velocity profiles, and minimising the velocity contamination (see for example the Ubertone’s ADVP, Conevski et al. 2020). The above consideration may be used in an attempt to explain the “banana”-like curved shape of the velocity profiles in Fig. 4c. Considering that for the flow examined herein the sweet spot is at about 50 mm from the face of the probe, Fig. 4c demonstrates capturing velocity profile measurements that deviate more from

the logarithmic profile the more distant from the sweet spot they are.

Generally, good results are found for sampling rates 25–50 Hz (e.g. Figure 4a), and even single point 1 mm velocimetry measurements at the sweet spot are found to be much better quality than the profiler results (Fig. 4c). Seeding of the flow should be sufficient so that the signal-to-noise ratio (SNR) will be around the range of 30–40 (especially around the sweet spot location). However, it needs be noted that the SNR was found to be highly dependent on the probe configuration. Thus, as a probe configuration is selected as being the optimal for the flow the seeding needs be checked to ensure sufficiently high SNR. In the experiments studied herein the flow is steady and boundary is fixed. However, for transient processes, such as seen in moving boundaries, e.g. over a wave induced flow field (Gaeta et al. 2020), high SNR and correlation may be indicative of a reflective boundary, implying that other means need be sought after (such as to analyse particles scattering and flow velocity spatiotemporal patterns in parallel with videography), and that high correlation is not an imperative goal (especially in cases where flow turbulence may be such where the acoustic pulses get to become uncorrelated).

Regarding the choice for the ping setting, it is thought that Adaptive ping may be preferable for cases of long-term deployment where the flow conditions may be changing or where there is no control or knowledge of the boundary of the flow. This works by sending relatively short space pings to estimate flow velocity and then trying to reduce the ping interval to match the velocity range, while considering the distance to the solid boundary. Minimal interval is a much preferable setting, where many more pings are sent over the same time period. Max interval is matching the interval of the pings to the velocity range of the measurements, using very long gap between the pings that gives the narrower velocity range that can be measured.

Dependance of the flow metrics on probe settings

As it is shown in Fig. 4 and Table 1, some experiments with high SNR and correlations but result in random velocity profile, and some results with relatively lower SNR and correlations provide more reasonable velocity profiles. For example, experiment 113114 has high averaged SNR (about 29 dB) and high averaged correlations (about 95%), however even the time series looks smooth and few spikes (Fig. 6a) and made the velocity profile random (Fig. 4). From those good-fit results, though the mean correlation remains above 85%, the mean SNR varies from 12 to 16 dB for some experiments (see Tables 2 and 4). The mean SNR values calculated with inclusion of the measurements at the near bed region, in which the echo from the boundary can increase the value of SNR, which means the averaged SNR for some

points is even smaller. Therefore, SNR and correlations cannot fully reflect the data quality.

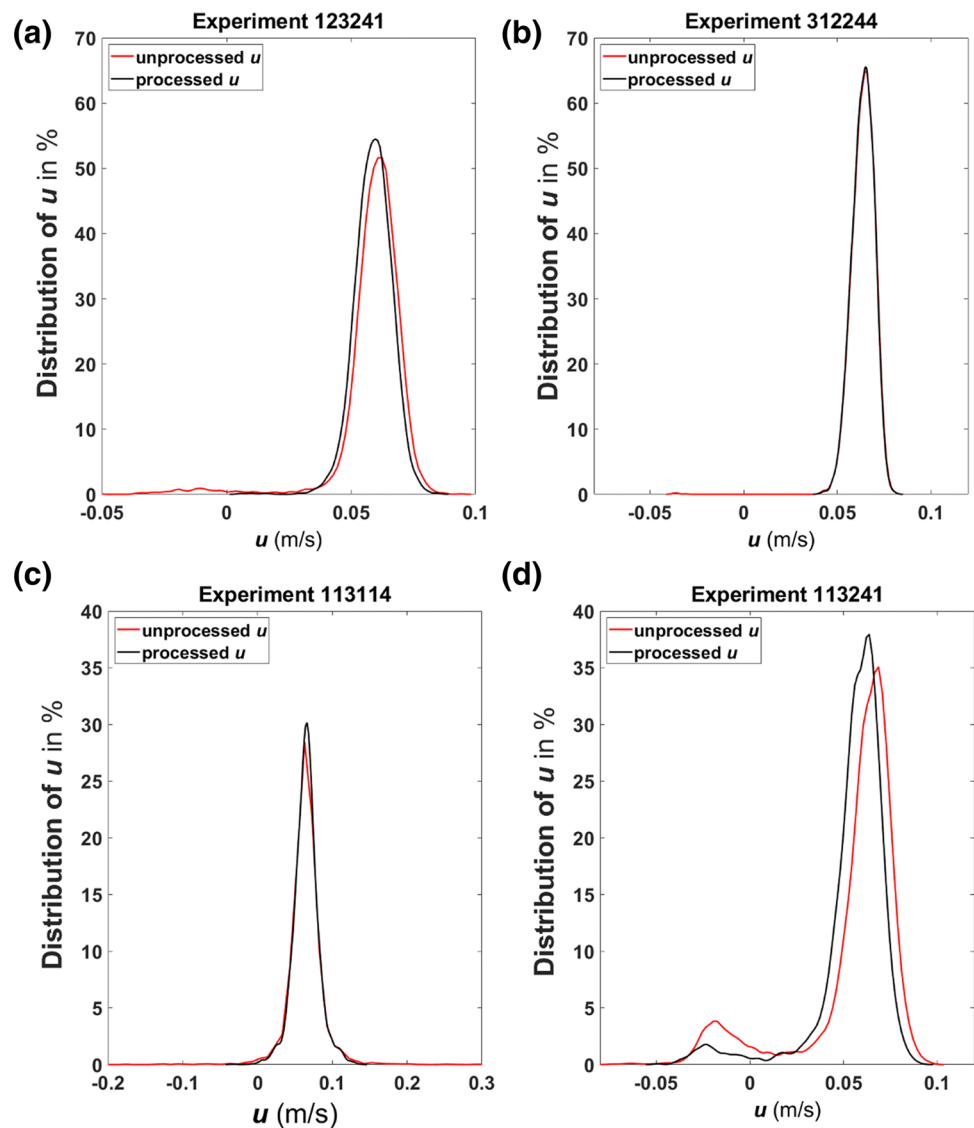
Table 4 also shows the mean percentage of spikes of all measurements in the profile with the specific probe configuration. Low SNR and correlations can result in the high percentage of spikes (Table 4), but they have negligible influence in the mean flow velocity calculated from the despiked velocity time series. All velocity data used in this study are after running the despiking code, which has little impact on the mean velocity calculation and the relevant analysis, such as velocity profile assessment and estimation of τ_{\log} . For instance, experiment 113241 has the maximum percentage of data points defined as spikes, but the averaged difference of the mean velocity is about 2×10^{-7} m/s (about 0.0003% of the mean velocity) before and after despiking (Fig. 6b), and for others among results that good-fit to a logarithmic function (e.g. Fig. 6c, d), this difference is much smaller.

Sampling rate is another key factor that affected the number of spikes, and the result shows that higher frequency of sampling rate can cause relatively more spikes in the velocity time series (Table 4). However, sampling rate does not have direct link to SNR and correlations, and this study also shows that the percentage of spikes is more sensitive to sampling rate. For example, experiment 111241 and 113241 contain 4.1% and 7.2% spikes, respectively, in which SNR and correlations of them are both small (see Table 2). In general, the number of spikes can be largely reduced by adding more seeding material (Khorsandi et al. 2012; NortekUSA 2011). In this experiment, the flow condition remains exactly same, so the percentage of spikes reflects the required minimum seeding concentration in the flow.

Meanwhile, the measured k_t is independent of the percentage of spikes. Both experiment 113241 and experiment 123241 have 7.2% spikes and similar SNR and correlations conditions, but more negative results can be observed in experiment 113241 (Fig. 6b, c), which do not significantly affect the mean velocity and velocity profile gradient (τ_{\log} for both are similar), but τ_{TKE} for 113241 is about three times of the τ_{TKE} for experiment 123241. The processed results for both experiment 123241 and 312244 have reasonable distribution of velocity (Fig. 6c, d), but the magnitude of k_t varies a lot, and the former is closer to τ_t . This indicates that metrics of SNR, Correlations (CC), and percentage of spikes while being indicative of the signal quality, they may not entirely be sufficient in representing how well the flow field is being sampled to produce reliable flow readings.

Both τ_{\log} and τ_{TKE} vary a lot, even they are only computed by the velocity profiles that are good-fit to a logarithmic function. For specific configurations of Vectrino II (like experiment 111241), τ_{TKE} is a few times higher than other probe configurations (such as experiment 111244 and 312244). The highest τ_{\log} is more than three times of the lowest. Comparing to the influence of spikes on hydrodynamic

Fig. 6 Distribution of unprocessed and processed instantaneous velocity time series at about 1/3 of the flow depth for the experiment with: **a** high SNR and correlations; **b** low SNR and correlations; **c** more spikes identified among the results well follow logarithmic functions; **d** less spikes identified among the results well follow logarithmic functions



variables, the impact of probe configuration is more significant. Thus, it is even more important to record velocity data with a good probe configuration than developing post-processing algorithms, because probe configurations can also significantly influence the mean velocity profile in addition to other computed results by using instantaneous velocities.

The time series of the flow velocity at a certain location could be obtained using acoustic Doppler velocimetry based on the acoustic principle. However, the instantaneous flow velocity readings are highly dependent on different parameters from the seeding to the probe configurations, depending on the flow conditions, as it has been shown in this work, which results in having uncertainties in the local flow velocities. The field of acoustic Doppler velocimetry has certain advantages over other velocimetry tools and one of its applications is the estimation of bed shear stress for the assessment of the destabilization of bed surface. The

bed shear stresses estimated using the flow velocity measurements is used to estimate the Shields stresses and hence assess the conditions that can result in sediment entrainment using the Shields criterion, or the Shields graph. However, there is a huge uncertainty in the assessment of riverbed destabilization using the Shields criterion due to the certainties discussed previously, the fact that the estimated bed shear stresses are dependent on the methodology used for their estimations (Yager et al. 2018), and the fact that the Shields criterion for sediment entrainment involves up to two orders of magnitude variability. Therefore, the use of other novel technologies, such as inertial sensors and instrumented pebbles (Al-Obaidi et al. 2020; Al-Obaidi and Valyrakis 2021a, b), allows for more robust assessment of bed surface destabilization directly and more efficiently than using Doppler-based flow velocimetry in addition to assessing the distribution of energetic flow structures sufficient

to mobilize sediments (Al-Obaidi and Valyrakis 2021a, b; Valyrakis et al. 2013).

Optimal probe configurations

No matter what changes for other indexes, all results show that Max Ping interval always made the SNR smaller than it with Adaptive Ping interval (Table 2). All profiles that fitted logarithmic functions follow the trend that for point-based measurements have larger values of p_1 and smaller p_2 comparing to those profile-based measurements. That results in both smaller τ_{\log} and smaller k_s . Cell size and Transmit pulse size should be treated carefully. If take the height of the mid-point of Cell size as the elevation of the measurement, the bed boundary affected region can become longer, however this is not clearly delivered in the user manual.

The four best probe configurations of Vectrino II are selected after assessing k_s , τ_{\log} and τ_{TKE} , and the velocity profiles are plotted in Fig. 7, which consists of two point-based measurements (experiment 111222 and 112244) and two profile-based measurements (experiment 411244 and 211222). The shape of the velocity profiles obtained by ADVP with these four probe configurations does not have big variation in p_1 and p_2 shown in Table 3. By using any of these four probe configurations, the recorded and computed flow hydrodynamic variables, such as mean velocity, τ_{\log} and k_t well agree to each other, which also shows a level of accuracy and consistency of Vectrino II.

This study shows a high level of dependency between probe configurations and velocity results, so depending on the type of analyses by the measured velocity, a test should be done to identify a proper probe configuration for the given flow condition before using Vectrino II. According to the aforementioned findings, Ping algorithm should be Max interval, and Range to first cell can be fixed either

40 mm or 50 mm, because it will not significantly affect the results. It is always preferred to choose high Sampling rate in many experimental works, however, a despiking algorithm may need to be run for configurations with high Sampling rate, which may cause more spikes along the unprocessed velocity time series. In addition, a note should be made that increasing either Cell size or Transmit pulse size may increase the length of boundary affected zone.

Framework for assessing optimal probe configurations

To identify an optimal probe configuration for near bed shear stress estimation under the given flow, the bed boundary influenced region should be detected first. Measurements within this region always have near zero velocity measurements in all directions and very high SNR with small fluctuations along the whole time series. At this region, the values of SNR for the four receiving beams do not match each other, and one or some of them are clearly higher. Measurements within this region do not reflect the actual flow velocity. Then, the quality of velocity time series needs to be evaluated. The time mean velocity after running an appropriate despiking algorithm should be almost the same as the raw mean velocity. Alternatively, the difference of the root-mean-square error between it for velocity time series processed once and twice should be negligible. The quality of the velocity profile can be assessed by comparing it with standard logarithmic functions. The smaller error indicates the higher quality of the profile. τ_{\log} and τ_{TKE} can be estimated separately, and the difference between τ_{\log} and τ_{TKE} is empirically suggested to be constantly smaller than 0.5 ($\tau_{\log} + \tau_{TKE}$). Benefits can also be obtained from comparing the computed result with the theoretical estimation of the near bed shear stress, if this is available.

Velocity profiles can be taken at the same location with different probe settings (choose a range of the values of profile length, Sampling rate, Cell size and Transmit pulse size depending on the aim and the requirement of the experiment, and test them). Visual check and check of fitness to a logarithmic function should be done. Analyses by using time mean velocities, such as depth mean velocity and shear stress estimated by the log Law of the Wall, can be achieved then. For analyses involving instantaneous velocities in time series, an additional analysis of turbulent kinetic energy (like comparing to the values of τ_{\log} and τ_{TKE}) is needed, and can follow the process demonstrated in this study. The percentage of spikes in the velocity time series does not significantly affect the time mean velocity, however it may influence the instantaneous velocity analyses in some extents, which can also be reflected by τ_{TKE} . So, shear stresses estimated by

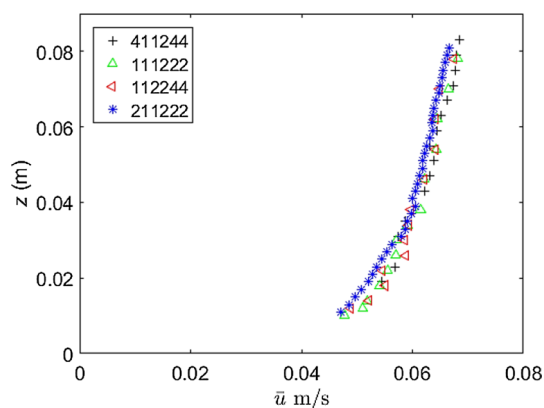


Fig. 7 Plots of velocity profiles for the best probe configurations assessed in this study. Because of the boundary effects, the profile starts from the sixth point from the channel bed

different methods with proper probe configurations should not vary a lot, and these values should well agree to them estimated from the theory.

Conclusions

Velocity profiles are taken at the same location and under the same flow condition by Vectrino II with different probe configurations. Although the production of the specific tested ADVP Vectrino II probe has been discontinued, these are still in use from a plethora of practitioners and researchers alike. Thus, it is expected that the practical findings regarding the specific probe configurations presented herein may still be of value, while caution is needed in using the proper velocimetry probe and settings for different flow dynamics and flow measurement circumstances. Analysis of the experimentally obtained results shows that the time-averaged flow velocity, τ_{\log} and τ_{TKE} vary significantly (the measured time-averaged velocity result can vary more than 50% of the mean flow velocity estimated from the flowrate, see Fig. 4; and the variation between the highest and the lowest shear stress can be up to 8 times, see Table 4), which shows that the sensitivity of the flow diagnostics to the probe configuration parameters needs be taken into account, before any measurements or estimations are attempted. The assessable metrics of data quality, SNR and correlations, suggested by the probe manufacture can only reflect the quality of velocity time series in certain level, in terms of number of spikes, but may not result in consistent measurements of the flow hydrodynamics. SNR and correlations are also sensitive to probe configurations. Given the inability of these metrics to offer a comprehensive understanding for the suitability of the probe configuration under a range of various settings, the use of a set of checks, flow metrics and estimated parameters, is demonstrated in assessing the optimal configuration. Specifically, comparing the shape of the obtained velocity profile to the expected (e.g. logarithmic, for wall bounded flows) can be performed by visual check. In addition to this, goodness of fit metrics to the expected theoretical velocity profile function can be also used. Computed values of τ_{TKE} from the instantaneous velocities, as well as values of τ_{\log} and k_s estimated from the velocity profiles, can be used to demonstrate the importance of carefully considering the optimal probe parameters. Some good probe configurations (for example those with sampling rates from 25 to 50 Hz, and single point measurement vs profiler measurement) are selected for the flow conditions assessed herein experimentally and the framework and metrics used to define these is presented. Certain trends can be observed from the analysis of the experiment results, consistent to the recent literature.

Adaptive Ping algorithm always leads to random velocity profiles (see Fig. 4d) and not preferable for normal wall-bounded flows with fixed boundaries. Min interval ping is preferable for flows up to 1.2 m/s. Point-based measurements always associate with lower SNR, and they result in smaller τ_{\log} and smaller k_s . Larger Cell size can make the boundary affected region longer. Overall, the probe's configuration parameters plays an important role on the accuracy of data obtained from Vectrino II, and this study offers a framework and metrics for assessing their optimal selection, following a set of focused pilot tests before the acquisition of experimental data for a given flow, as demonstrated in this study for specific flow conditions.

Funding This research has been supported by the Royal Society (Research Grant RG2015 R1 68793/1), the Royal Society of Edinburgh (Crucible Award), and the Carnegie Trust for the Universities of Scotland (project 7066215).

Data availability The data that support the findings of this study are available on request from the corresponding author.

Declarations

Conflict of interest The authors declare that they have no conflict of interest.

Open Access This article is licensed under a Creative Commons Attribution 4.0 International License, which permits use, sharing, adaptation, distribution and reproduction in any medium or format, as long as you give appropriate credit to the original author(s) and the source, provide a link to the Creative Commons licence, and indicate if changes were made. The images or other third party material in this article are included in the article's Creative Commons licence, unless indicated otherwise in a credit line to the material. If material is not included in the article's Creative Commons licence and your intended use is not permitted by statutory regulation or exceeds the permitted use, you will need to obtain permission directly from the copyright holder. To view a copy of this licence, visit <http://creativecommons.org/licenses/by/4.0/>.

References

- Al-Obaidi K, Xu Y, Valyrakis M (2020) The design and calibration of instrumented particles for assessing water infrastructure hazards. *J Sens Actuator Netw* 9(3):36
- Al-Obaidi K, Valyrakis M (2021a) A sensory instrumented particle for environmental monitoring applications: development and calibration. *IEEE Sens J* 21(8):10153–10166
- Al-Obaidi K, Valyrakis M (2021) Linking the explicit probability of entrainment of instrumented particles to flow hydrodynamics. *Earth Surf Process Landf* 46:2448–2465
- Anderson S, Lohrmann A (1995) Open water test of the Sontek acoustic Doppler velocimeter. In: St. Petersburg, IEEE fifth working conf. on current measurements. *IEEE J Ocean* pp 188–192
- Biron PM, Robson C, Lapointe MF, Gaskin SJ (2004) Comparing different methods of bed shear stress estimates in simple and complex flow fields. *Earth Surf Process Landf* 29(11):1403–1415. <https://doi.org/10.1002/esp.1111>

- Camenen B, Larson M, Bayram A (2009) Equivalent roughness height for plane bed under oscillatory flow. *Estuarine Estuar* 81(3):14p
- Conevski S, Aleixo R, Guerrero M, Ruther N (2020) Bedload velocity and backscattering strength from mobile sediment bed: a laboratory investigation comparing bistatic versus monostatic acoustic configuration. *Water* 12(12):3318. <https://doi.org/10.3390/w12123318>
- Gaeta MG, Guerrero M, Formentin SM, Palma G, Zanuttigh B (2020) Non-intrusive measurements of wave-induced flow over dikes by means of a combined ultrasound doppler velocimetry and videography. *Water* 12(11):3053. <https://doi.org/10.3390/w12113053>
- Craig RG, Loadman C, Clement B, Rusello PJ, Siegel E (2010) Characterization and testing of a new bistatic profiling acoustic doppler velocimeter: the Vectrino-II. In: Proceedings of the IEEE/OES/CWTM tenth working conference on current measurement technology, pp 246–252
- García CM, Cantero MI, Niño Y, García MH (2005) Turbulence measurements with acoustic Doppler velocimeters. *J Hydraul Eng* 131(12):1062–1073. [https://doi.org/10.1061/\(ASCE\)0733-9429\(2005\)131:12\(1062\)](https://doi.org/10.1061/(ASCE)0733-9429(2005)131:12(1062))
- Goring DG, Nikora VI (2002) Despiking acoustic doppler velocimeter data. *J Hydraul Eng* 128(1):117–126. [https://doi.org/10.1061/\(ASCE\)0733-9429\(2002\)128:1\(117\)](https://doi.org/10.1061/(ASCE)0733-9429(2002)128:1(117))
- Hurther D, Lemmin U (2001) A correction method for turbulence measurements with a 3D acoustic Doppler velocity profiler. *J Atmos Ocean Technol* 18:446–458. [https://doi.org/10.1175/1520-0426\(2001\)018%3c0446:ACMFTM%3e2.0.CO;2](https://doi.org/10.1175/1520-0426(2001)018%3c0446:ACMFTM%3e2.0.CO;2)
- Jesson M, Bridgeman J, Sterling M (2015) Novel software developments for the automated post-processing of high volumes of velocity time-series. *Adv Eng Softw* 89:36–42. <https://doi.org/10.1016/j.advengsoft.2015.06.007>
- Jesson M, Sterling M, Bridgeman J (2013) Despiking velocity time-series—optimisation through the combination of spike detection and replacement methods. *Flow Meas Instrum* 30:45–51. <https://doi.org/10.1016/j.flowmeasinst.2013.01.007>
- Khorsandi B, Mydlarski L, Gaskin S (2012) Noise in turbulence measurements using acoustic Doppler velocimetry. *J Hydraul Eng* 138(10):829–838
- Kraus NC, Lohrmann A, Cabrera R (1994) New acoustic meter for measuring 3D laboratory flows. *J Hydraul Eng* 120(3):406–412. [https://doi.org/10.1061/\(ASCE\)0733-9429\(1994\)120:3\(406\)](https://doi.org/10.1061/(ASCE)0733-9429(1994)120:3(406))
- McLelland SJ, Nicholas AP (2000) A new method for evaluating errors in high-frequency ADV measurements. *Hydrol Process* 14(2):351–366. [https://doi.org/10.1002/\(SICI\)1099-1085\(20000215\)14:2%3c351::AID-HYP963%3e3.0.CO;2-K](https://doi.org/10.1002/(SICI)1099-1085(20000215)14:2%3c351::AID-HYP963%3e3.0.CO;2-K)
- NortekAS (2012) Vectrino profiler user guide. Nortek Scientific Acoustic Development Group Inc., Boston
- NortekAS (2015) Comprehensive manual. Available at: <http://www.nortek-as.com/lib/manuals/the-comprehensive-manual>. Accessed 22 Oct 2017
- NortekUSA (2011) Vectrino II Configuration. Available at: <http://www.nortekusa.com/usa/knowledge-center/table-of-contents/vectrino-ii/configuration>. Accessed 9 Oct 2017
- NortekUSA (2011) Velocimeters-principles of operation: acoustic doppler velocimeters. Available at: <http://www.nortekusa.com/usa/knowledge-center/table-of-contents/velocimeters>. Accessed 12 October 2017.
- Parsheh M, Sotiropoulos F, Porté-Agel F (2010) Estimation of power spectra of acoustic-Doppler velocimetry data contaminated with intermittent spikes. *J Hydraul Eng* 136(6):368–378. [https://doi.org/10.1061/\(ASCE\)HY.1943-7900.0000202](https://doi.org/10.1061/(ASCE)HY.1943-7900.0000202)
- Rusello P (2012) Near boundary measurements with a profiling acoustic Doppler velocimeter. In: HMEM conference August 12–15 2012, Snowbird, UT.
- Sumer B (2007) Lecture Notes on Turbulence. Available at: http://www.external.mek.dtu.dk/personal/bms/turb_book_update_30_6_04.pdf. Accessed 9 October 2017.
- Thomas R, Schindfessel L, McLelland S, Creele S (2017) Bias in mean velocities and noise in variances and covariances measured using a multistatic acoustic profiler: the Nortek Vectrino Profiler. *Meas Sci Technol* 28(7):075302. <https://doi.org/10.1088/1361-6501/aa7273>
- Valyrakis M, Diplas P, Dancy CL (2013) Entrainment of coarse particles in turbulent flows: an energy approach. *J Geophys Res Earth Surf* 118(1):42–53. <https://doi.org/10.1029/2012JF002354>
- Voulgaris G, Trowbridge JH (1998) Evaluation of the acoustic Doppler velocimeter (ADV) for turbulence measurements. *J Atmos Ocean Technol* 15:272–289
- Yager EM, Venditti JG, Smith HJ, Schmeeckle MW (2018) The trouble with shear stress. *Geomorphology* 323:41–50
- Yang JQ, Chung H, Nepf HM (2016) The onset of sediment transport in vegetated channels predicted by turbulent kinetic energy. *Geophys Res Lett*. <https://doi.org/10.1002/2016GL071092>
- Zedel L, Hay A (2011) Turbulence measurements in a jet: comparing the Vectrino and VectrinoII. In: Proceedings of the IEEE/OES/CWTM tenth working conference on current measurement technology, Monterey, Canada, pp 173–178